Radboud Universiteit

GRAPHENE FLAGSHIP

Theory of carbon-based magnetism

Mikhail Katsnelson

Theory of Condensed Matter
Institute for Molecules and Materials
RU

Outline

- *sp* magnetism in general: why it is interesting?

- Defect-induced magnetism in graphene: Lieb theorem, midgap states, and all that

- Zigzag edges, *g*rain boundaries, carbon foam, defected fullerenes...

- Exotic magnetism in C_2H and C_2F

Magnetism of *sp* electrons in narrow impurity bands: Model considerations

D.M.Edwards & MIK, JPCM 18, 7209 (2006)

Motivation: "semi-reproducible" magnetism in carbon systems, CaB_6, etc.: defect-related

Theoretically: any essential difference with Fe, Co, Ni itinerant-electron magnetism? Yes!!! Possible way to high Curie temps.

Two main differences

Standard itinerant-electron ferromagnets:

- Strong suppression of Stoner parameter by correlation renormalizations (Kanamori)
- T_C is determined by spin waves rather than Stoner excitations

If Fe would be Stoner magnet it would have $T_C \approx 4000\ K$ (in reality 1043 *K*)

***sp*- electron itinerant electron FMs are Stoner magnets and thus can have much higher T_C than usual dilute magnetic semiconductors**

Stoner criterion

$$I_{\mathrm{eff}} N\left(E_{\mathrm{F}}\right) > 1$$

$N(E_{\mathrm{F}})$ is the density of one-electron states

I_{eff} is an on-site interaction parameter

Equation for the Curie temperature:

$$I_{\mathrm{eff}} \int \mathrm{d}E \left(-\frac{\partial f}{\partial E}\right) N(E) = 1$$

***f(E)* Fermi function**

Rectangular band, width W_{imp}:

$$k_{\mathrm{B}} T_{\mathrm{c}} = W_{\mathrm{imp}} / \left[4 \tanh^{-1}\left(W_{\mathrm{imp}} / I_{\mathrm{eff}} n_{\mathrm{imp}}\right)\right]$$

$$k_{\mathrm{B}} T_{\mathrm{c}} < I_{\mathrm{eff}} n_{\mathrm{imp}} / 4$$

Stoner parameter ≈ 1eV

Room-temperature FM:

n_{imp} > 0.01

Kanamori renormalization

T-matrix: $I_{eff} \approx I / [1 + const\ I/W]$

Usually (Fe, Co, Ni…) Stoner criterion satisfies at the border $I_{eff} N(E_F) \approx 1.2$.

Impurity bands: T-matrix renormalization can be unusually small due to spectral weight transfer effects

General theory of T-matrix renormalization

Hamiltonian

$$H = H_{\mathrm{t}} + H_{\mathrm{U}}$$

$$H_{\mathrm{t}} = \sum_{\lambda\lambda'\sigma} t_{\lambda\lambda'} c^{\dagger}_{\lambda\sigma} c_{\lambda'\sigma}$$

$$H_{\mathrm{U}} = \frac{1}{2} \sum_{\{\lambda_i\}\sigma\sigma'} \left\langle \lambda_1 \lambda_2 \left| v \right| \lambda'_1 \lambda'_2 \right\rangle c^{\dagger}_{\lambda_1\sigma} c^{\dagger}_{\lambda_2\sigma'} c_{\lambda'_2\sigma'} c_{\lambda'_1\sigma}$$

Equation for T-matrix

$$\langle 13 | T^{\sigma\sigma'} (\mathrm{i}\Omega) | 24 \rangle = \langle 13 | v | 24 \rangle - \frac{1}{\beta} \sum_{\omega} \sum_{5678} \langle 13 | v | 57 \rangle \, G^{\sigma}_{56} (\mathrm{i}\omega) \times G^{\sigma'}_{78} (\mathrm{i}\Omega - \mathrm{i}\omega) \langle 68 | T^{\sigma\sigma'} (\mathrm{i}\Omega) | 24 \rangle,$$

$\omega = (2n + 1)\pi k_{\mathrm{B}} T$ are the Matsubara frequencies

General theory of T-matrix renormalization *II*

Spectral representation:

$$G^{\sigma}_{56}(i\omega) = \int_{-\infty}^{\infty} \mathrm{d}x \, \frac{\rho_{56}(x)}{\mathrm{i}\omega - x}$$

On-site (Hubbard) interaction)

$$\langle 13|T(E)|24\rangle = \langle 13|v|24\rangle + \sum_{5678} \langle 13|v|57\rangle \langle 57|P(E)|68\rangle \langle 68|T(E)|24\rangle$$

$$\langle 57|P(E)|68\rangle = \int_{-\infty}^{\infty} \mathrm{d}x \int_{-\infty}^{\infty} \mathrm{d}y \frac{1 - f(x) - f(y)}{E - x - y} \rho_{56}(x)\rho_{78}(y)$$

Conventional itinerant-electron FM vs impurity-band FM

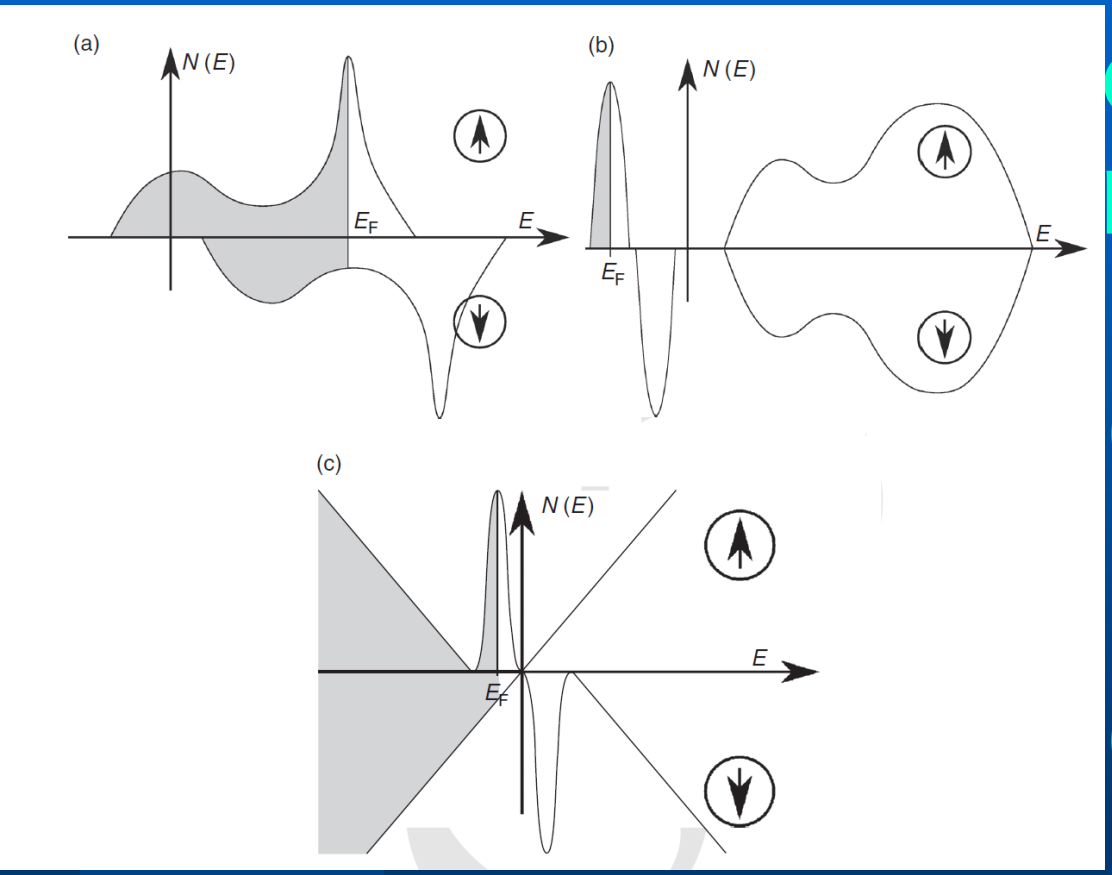

One-band FM, weak polarization

Broad main band (region *I*)

Impurity band (region *II*)

Fig. 12.1. A sketch of the electronic structures for various types of itinerant-electron ferromagnet: (a) the conventional case; (b) and (c) defect-induced half-metallic ferromagnetism in semiconductors and in graphene, respectively.

FM in impurity bands

$$\int_{\mathrm{I}}\int_{\mathrm{I}} \frac{\mathrm{d}x\,\mathrm{d}y}{x+y}\rho\,(x)\,\rho\,(y) \sim \frac{1}{W} Z^2_{\mathrm{band}},$$

$$\int_{\mathrm{II}}\int_{\mathrm{II}} \frac{\mathrm{d}x\,\mathrm{d}y}{x+y}\rho\,(x)\,\rho\,(y) \sim \frac{1}{W_{\mathrm{imp}}} Z^2_{\mathrm{imp}},$$

$$\int_{\mathrm{I}}\int_{\mathrm{II}} \frac{\mathrm{d}x\,\mathrm{d}y}{x+y}\rho\,(x)\,\rho\,(y) \sim \frac{1}{W} \ln\left(\frac{W}{W_{\mathrm{imp}}}\right) Z_{\mathrm{band}} Z_{\mathrm{imp}}.$$

$$Z_{\mathrm{imp}} = \int_{\mathrm{II}} \mathrm{d}x\;\rho(x),$$

$$Z_{\mathrm{band}} = \int_{\mathrm{I}} \mathrm{d}x\;\rho(x) = 1 - Z_{\mathrm{imp}}$$

Shallow imputities:
Z_{imp} « 1
which suppress suppression of *I*

Magnon stiffness constant in impurity – band FM

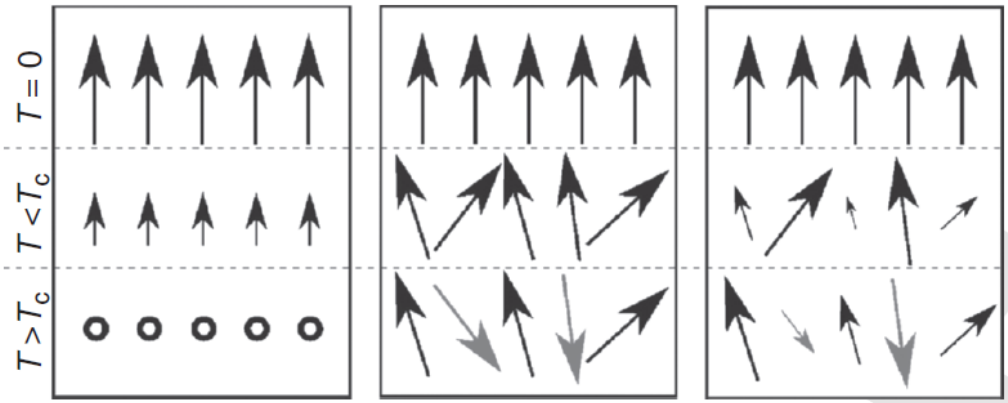

Fig. 12.3. The temperature evolution of ferromagnetic states in the Stoner model (left panel), in the Heisenberg model (middle panel) and in real itinerant-electron ferromagnets (right panel).

Exchange integrals through local rotations

$$c_{im} \rightarrow U(\theta_i, \varphi_i)\, c_{im}$$

where

$$U(\theta, \varphi) = \begin{pmatrix} \cos\theta/2 & \sin\theta/2 \exp(-i\varphi) \\ -\sin\theta/2 \exp(i\varphi) & \cos\theta/2 \end{pmatrix}$$

$$\theta_i = const \text{ and } \varphi_i = \mathbf{qR_i}$$

Magnon stiffness constant in impurity – band FM *II*

$$\delta H = \sum_{ij} Tr_{L\sigma}\left[t_{ij} c_i^+ \left(U_i^+ U_j - 1\right) c_j\right] = \delta_1 H + \delta_2 H$$

$$\delta_1 H = \sin^2\frac{\theta}{2} \sum_k Tr_{L\sigma}\left[\left(t\left(\mathbf{k}+\mathbf{q}\right) - t\left(\mathbf{k}\right)\right) c_{\mathbf{k}}^+ c_{\mathbf{k}}\right]$$

$$\delta_2 H = \frac{1}{2}\sin\theta \sum_{ij} Tr_L\left[t_{ij} c_{i\downarrow}^+ c_{j\uparrow}\right]\left(\exp\left(i\mathbf{q}\mathbf{R}_i\right) - \exp\left(i\mathbf{q}\mathbf{R}_j\right)\right)$$

Perturbation theory up to θ^2 with local self-energy (the only approximation)

Magnon stiffness constant in impurity – band FM *III*

$$D = \frac{1}{6\pi\,(n_\uparrow - n_\downarrow)}\,\mathrm{Im}\int_{-\infty}^{E_\mathrm{F}} \mathrm{d}E \sum_{\mathbf{k}} \left[G^{\uparrow}_{\mathbf{k}}(E) - G^{\downarrow}_{\mathbf{k}}(E)\right]^2 |\nabla_{\mathbf{k}}\epsilon\,(\mathbf{k})|^2$$

RPA value of the stiffness constant:

$$D_0 = -\frac{R^2}{6\,(n_\uparrow - n_\downarrow)}\,\langle H_0\rangle = \frac{1}{12}R^2 W$$

Estimation for simplest model, NN hopping

$$D = D_0 + D_1 \simeq \frac{1}{9}\frac{\hbar^2}{2m^*} = \frac{1}{9}D_0$$

no smallness in electron concentration!

Magnon energies are higher than the Fermi energy of electrons!

- **normal itinerant- electron magnets: easier to rotate spins than to change their length**
- ***sp*-magnets: Stoner magnets (after *70 years of existence of the Stoner model a region of applicability was found)***

Vacancies and other sp^3 defects

Lieb theorem: Hubbard model for bipartite lattice

$$\hat{H} = \sum_{ij\sigma} t_{ij} \hat{c}^{+}_{i\sigma} \hat{c}_{j\sigma} + U \sum_{i} \hat{n}_{i\uparrow} \hat{n}_{i\downarrow}$$

$$\hat{t}_{\mathrm{AA}} = \hat{t}_{\mathrm{BB}} = 0$$

NN approx.

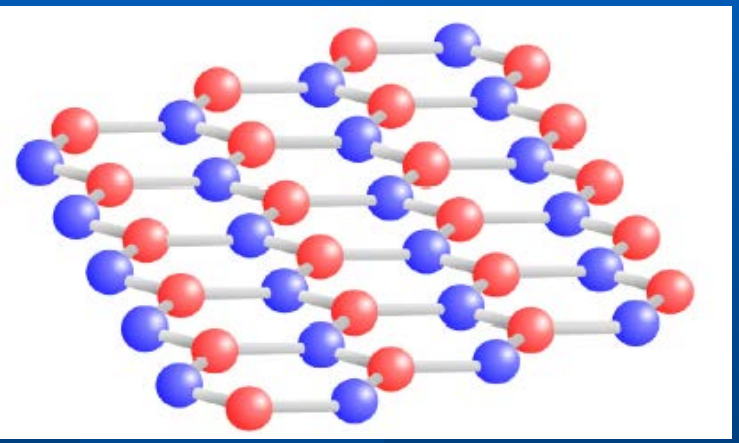

Two equivalent sublattices, A and B (pseudospin)

N_{A} and N_{B} Number of sites in sublattices

The ground state spin: $$S = \frac{N_{\mathrm{B}} - N_{\mathrm{A}}}{2}$$ Lieb, PRL 1989

Vacancies and other sp^3 defects II

- Mid-gap states lead to (local) spin polarization
  - FM exchange in the same sublattice, AFM between A and B
  - Hydrogen and other sp^3 defects act very similar to vacancies

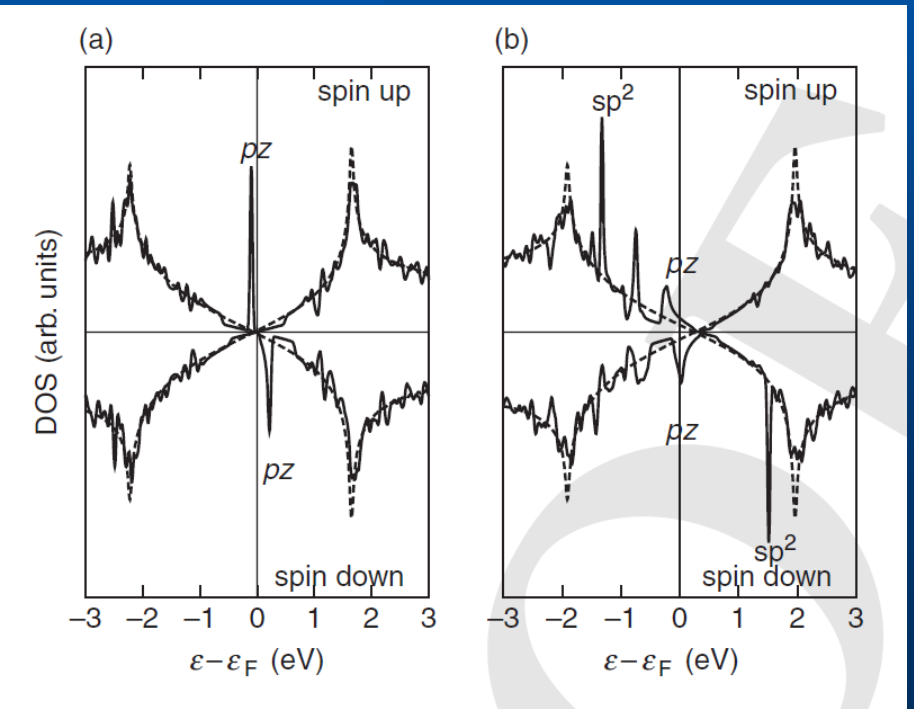

(a) H adatom
(b) Vacancy

Yazyev & Helm, PRB 2007

Vacancies and other sp^3 defects III

Dual origin of defect magnetism in graphene and its reversible switching by molecular doping

R.R Nair[1], I-L Tsai[1], M. Sepioni[1], O. Lehtinen[2], J. Keinonen[2], A.V Krasheninnikov[2,3], A.H Castro Neto[4], M.I Katsnelson[5], A.K Geim[1] & I.V Grigorieva[1]

NATURE COMMUNICATIONS | 4:2010 | DOI: 10.1038/ncomms3010

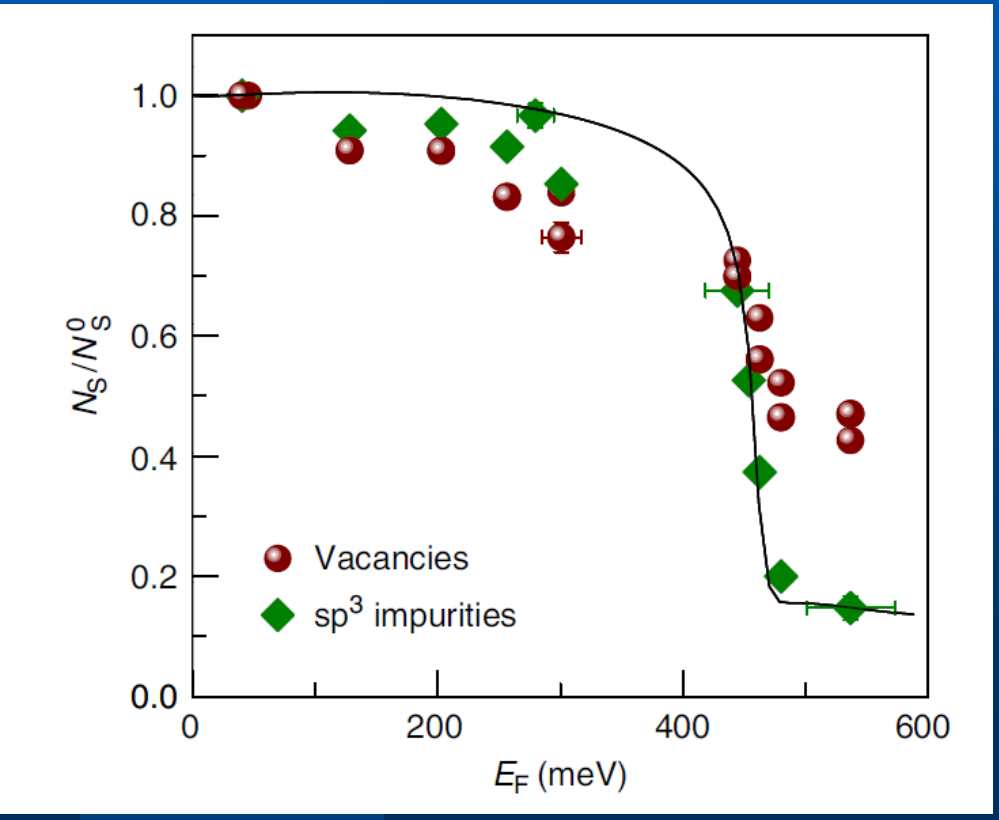

Vacancies: two types of LMM: π (midgap states) and σ (dangling bonds); admolecules: only π

No signs of magnetic order!!!

Polymerized fullerenes

A very controversial issue (experimentally)

D.W. Boukhvalov & MIK, EPJ B 68, 529 (2009)

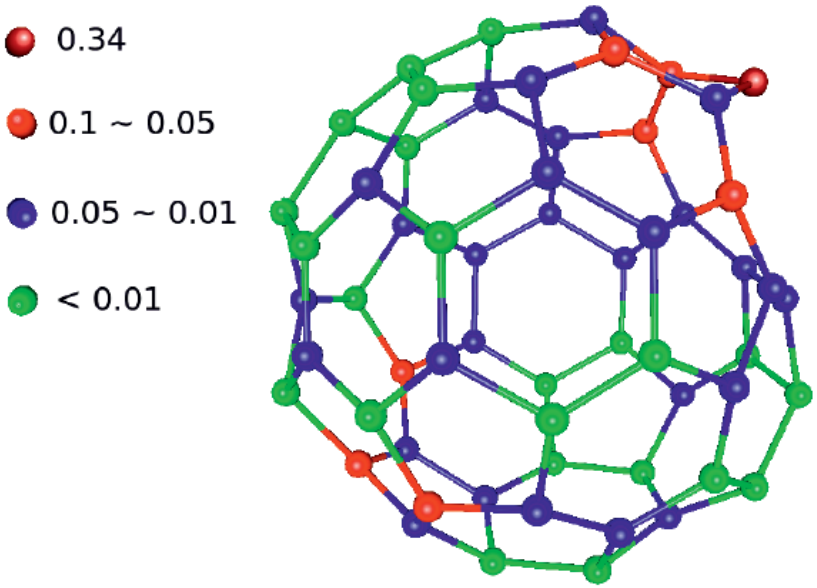

Fig. 4. (Color online) Distribution of magnetic moments in μ_B on C_{60} sphere with single vacancy in rhombohedral phase.

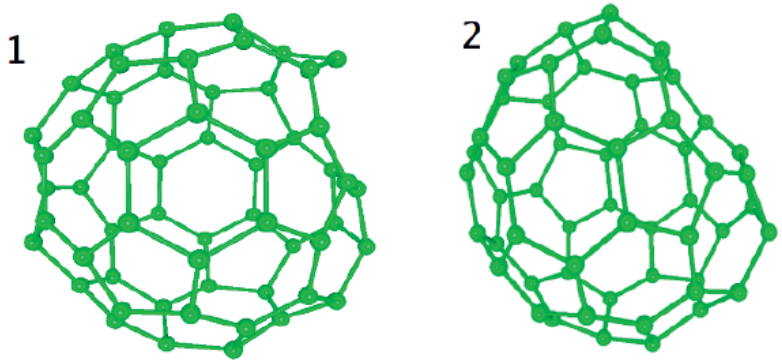

Bivacancy (2) is nonmagnetic and more favourable (2 eV per atom lower)

Single vacancy is magnetic

Effect of vacancies/adatoms: QMC

M. Ulybyshev & MIK, PRL 114, 246801 (2015)

Random missing sites equally distributed in two sublattices

AFM state with very strong exchange interactions

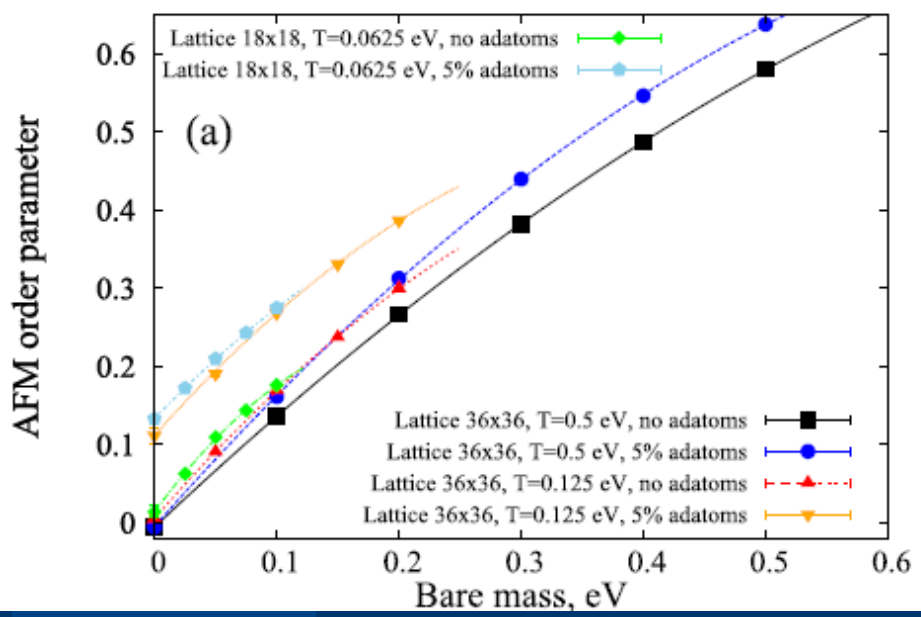

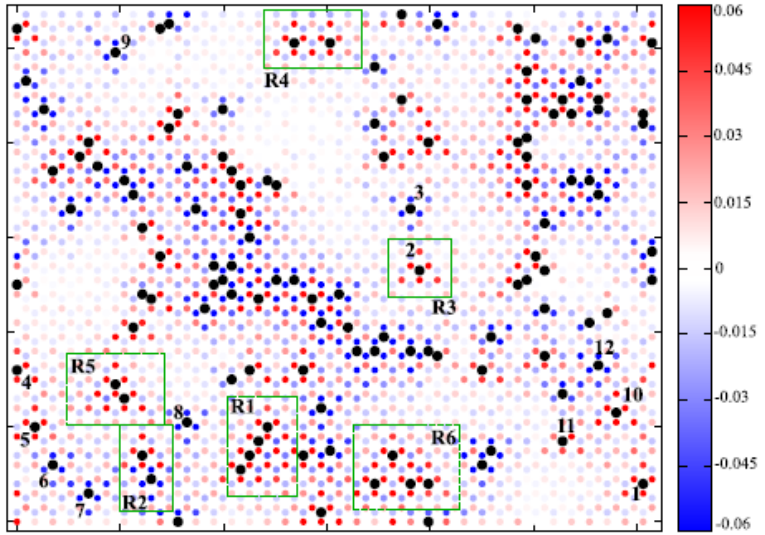

FIG. 2 (color online). Distribution of average spin. The color scale corresponds to $\langle S_z \rangle$ at a site in the zero bare mass limit.

Lieb theorem works for long-range interactions...

Effect of vacancies/adatoms II

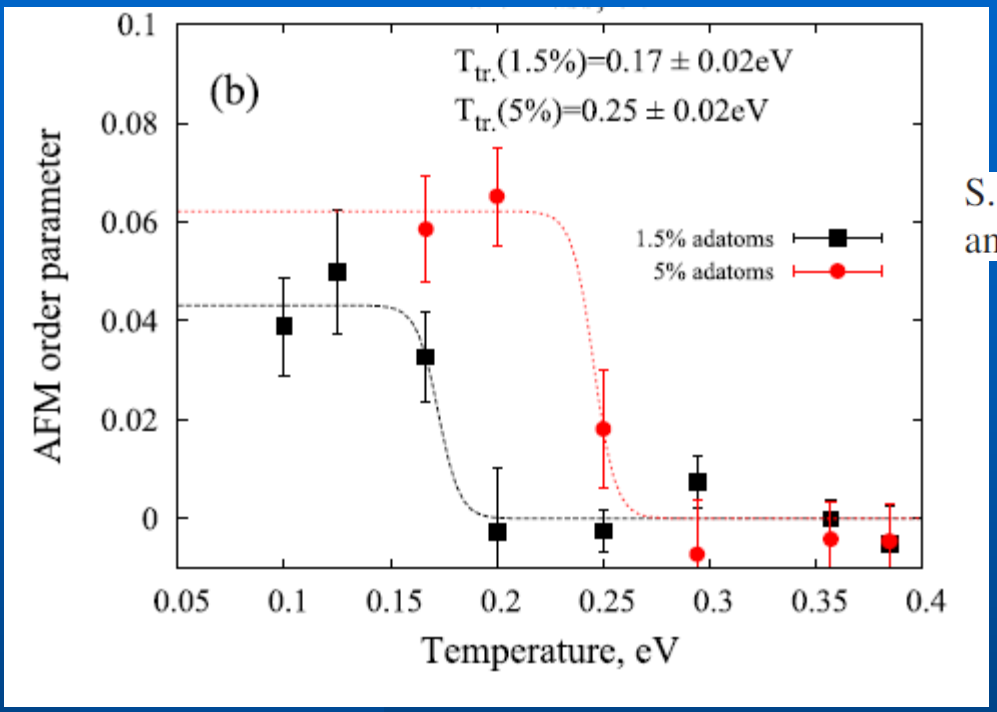

For vacancies: clearly contradict experiments

S. Just, S. Zimmermann, V. Kataev, B. Büchner, M. Pratzer, and M. Morgenstern, Phys. Rev. B **90**, 125449 (2014).

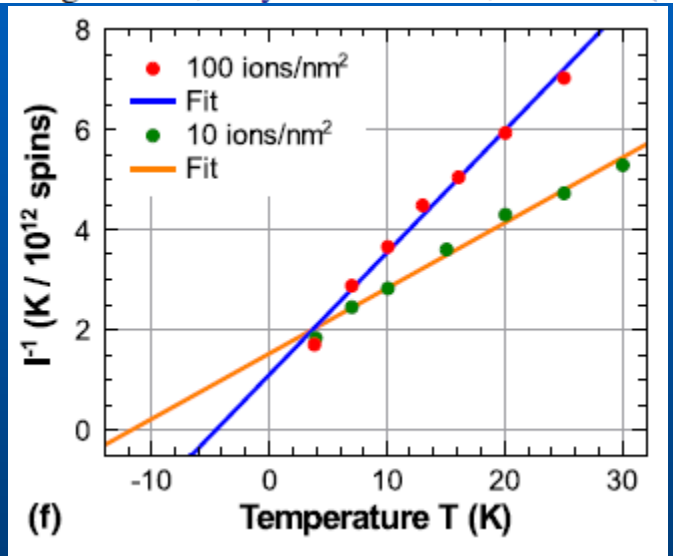

(f) Temperature-dependent inverse peak area of the ESR curves calibrated by a ruby standard (see text) in comparison with fit curves $a(T - \theta_{cw})$ revealing $\theta_{cw} = -12$ K and $\theta_{cw} = -5$ K, respectively.

Model of empty sites gives too srong antiferromagnetic exchange

Effect of vacancies/adatoms III

nature physics

LETTERS

PUBLISHED ONLINE: 10 JANUARY 2012 | DOI: 10.1038/NPHYS2183

Spin-half paramagnetism in graphene induced by point defects

R. R. Nair[1], M. Sepioni[1], I-Ling Tsai[1], O. Lehtinen[2], J. Keinonen[2], A. V. Krasheninnikov[2,3], T. Thomson[1], A. K. Geim[1] and I. V. Grigorieva[1]*

both scarce and controversial[13–16]. Here we show that point defects in graphene—(1) fluorine adatoms in concentrations x gradually increasing to stoichiometric fluorographene $CF_{x=1.0}$ (ref. 17) and (2) irradiation defects (vacancies)—carry magnetic moments with spin 1/2. Both types of defect lead to notable paramagnetism but no magnetic ordering could be detected down to liquid helium temperatures. The induced paramagnetism dominates graphene's low-temperature magnetic properties, despite the fact that the maximum response we could achieve was limited to one moment per approximately 1,000 carbon atoms. This limitation is explained by

For fluorinated graphene: mostly no local moments (or very high AFM coupling between them)

For vacancies: quite strong distortion, buckling etc., other rlectron states are involved

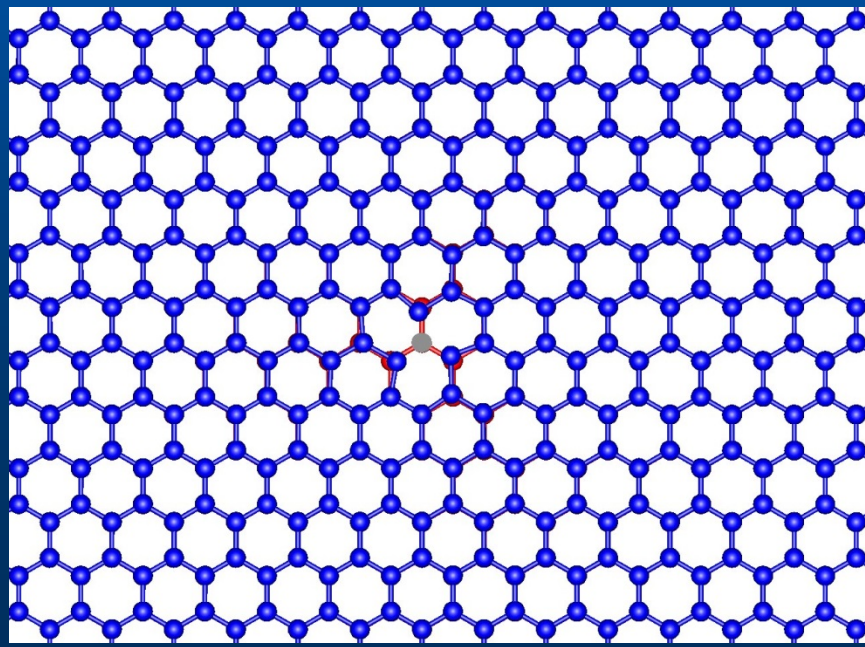

Effect of vacancies/adatoms IV

Gap opening dut to Coloumb interaction

	Center 1	Width 1	Center 2	Width 2	Gap
Ordinary potentials	0.76	0.40	-0.69	0.22	1.1 ± 0.17
Screened potentials	0.52	0.16	-0.49	0.18	0.74 ± 0.12

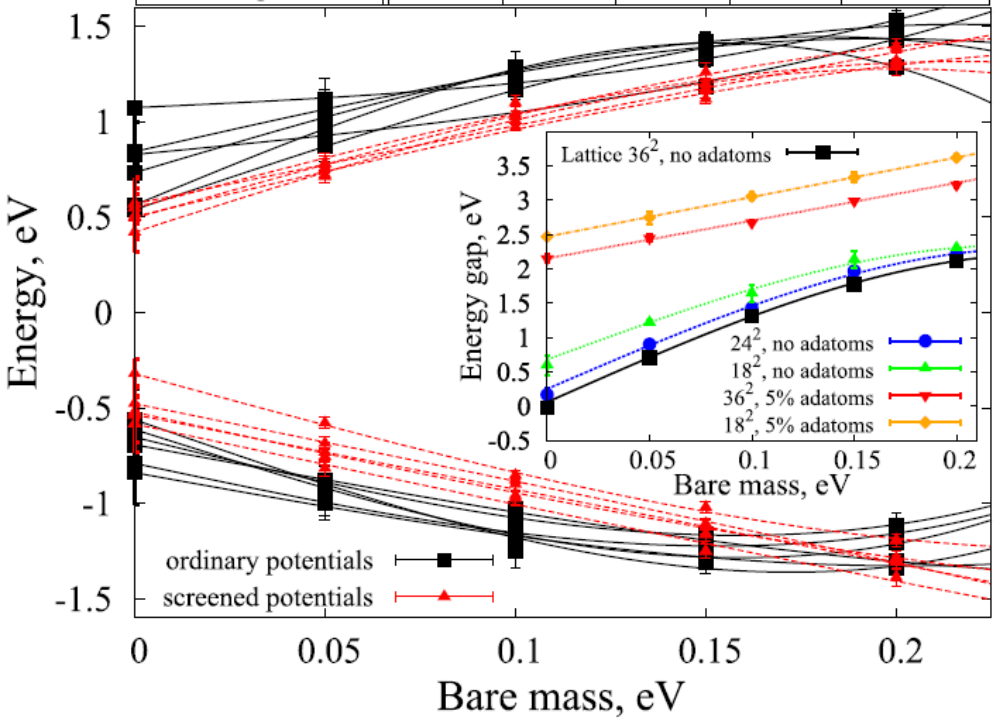

FIG. 3 (color online). Energies of the midgap states for two sets of interelectron potentials. Each state corresponds to one isolated vacancy marked with the number in Fig. 2. The center and width of the bands are calculated in the limit $m \to 0$. The center is the average over the energies of all states in each band and the width is equal to the doubled dispersion. $T = 0.125$ eV. The real physical situation is restored in the limit $m \to 0$. Inset: energy gap between normal energy bands. All values correspond to the K point in the Brillouin zone.

Quite noticeable gap in impurity band and much larger in K point for freely suspended graphene with 5% defects.

Can be measured optically

Magnetism at zigzag edges

Half-metallic graphene nanoribbons

Young-Woo Son[1,2], Marvin L. Cohen[1,2] & Steven G. Louie[1,2]

Nature 444, 347 (2006)

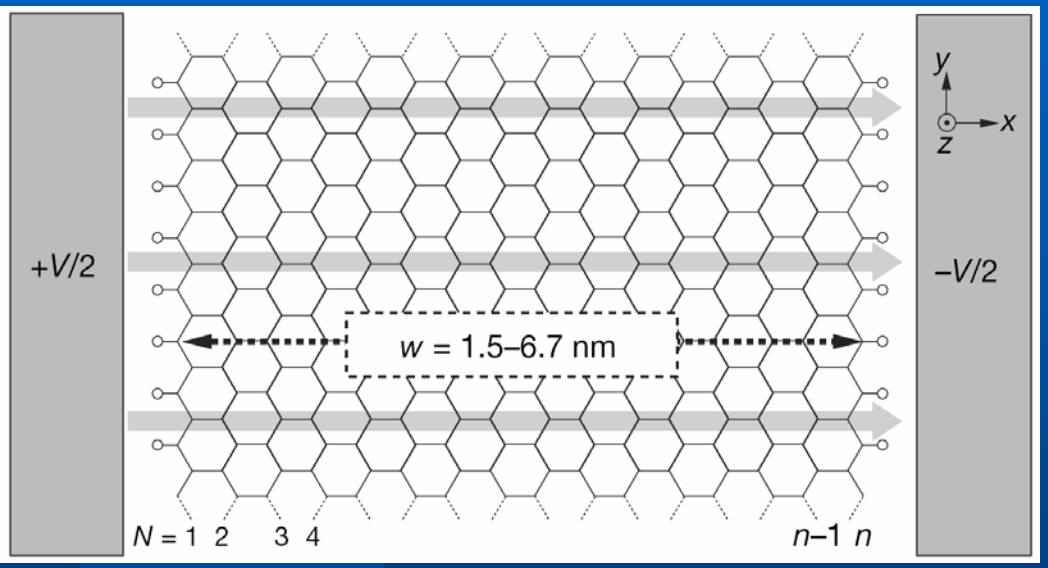

Zigzag edges: midgap states in nonmagnetic case (true in a generic case as well)

Spin polarization arises

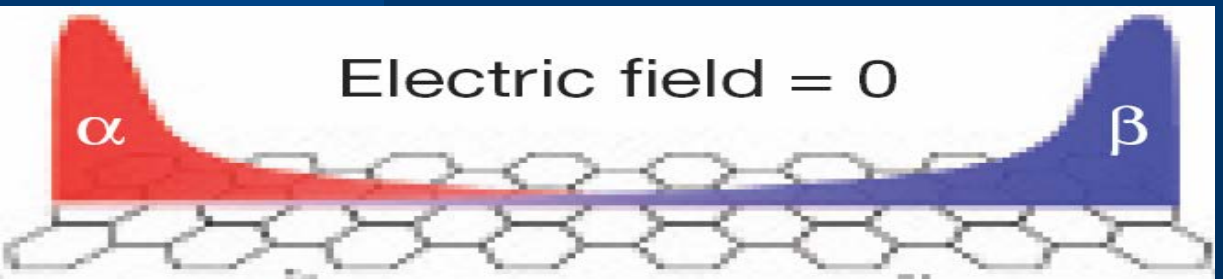

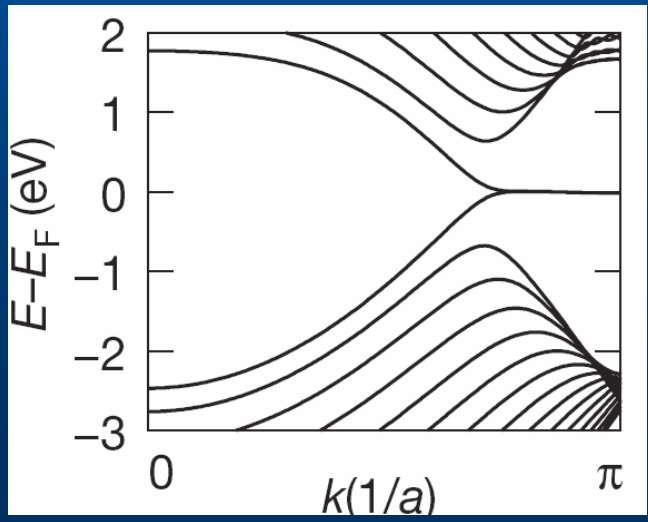

Magnetism at zigzag edges II

1D systems: no magnetic ordering at finite T

Exchange interactions and finite-T magnetism

Yazyev & MIK PRL 100, 047209 (2008)

Energies of transverse (a) and longitudinal (b) configurations, DFT-SIESTA calculations

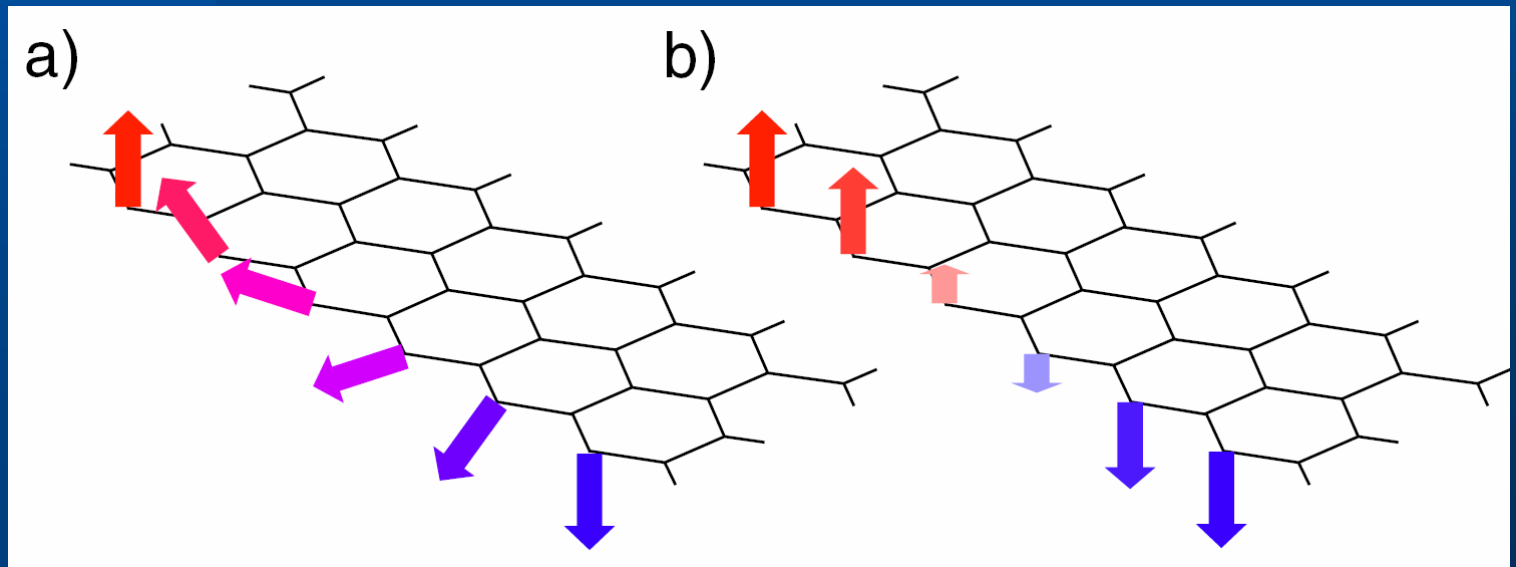

Magnetism at zigzag edges III

A very high spin stiffness constant

$$D = 2100 \text{ meV Å}^2$$

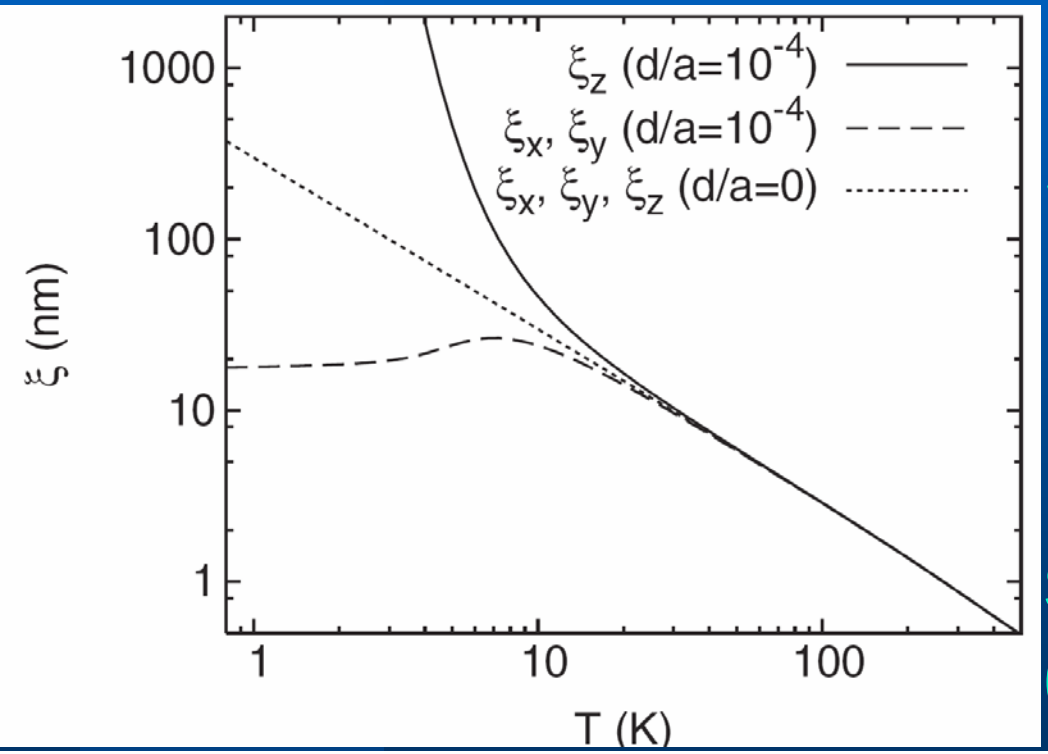

FIG. 3. Correlation lengths of magnetization vector components orthogonal (ξ_z) and parallel (ξ_x, ξ_y) to the graphene plane as a function of temperature T for weakly anisotropic ($d/a = 10^{-4}$) and isotropic ($d/a = 0$) Heisenberg models.

@ RT:
Superparamagnetism
Enhancement factor 8

Low temperatures:
spin coherence at
0.1 μm

Magnetism at zigzag edges IV

Bhandary, Eriksson, Sanyal & MIK, PRB 82, 165405 (2010)

Double-hydrogenated zigzag edges in nanoribbons: still ferromagnetic!

TABLE I. Difference in total energies between the nonmagnetic and ferromagnetic states (ΔE) and the corresponding magnetic moments in the ferromagnetic state. The energy differences and total magnetic moments are quoted for the unit cell whereas the edge moment is for one C atom at the edge.

Width (rows)	ΔE (meV)	Total moment (μ_B)	Edge moment (μ_B)
8	1.63	1.04	0.34
10	5.3	1.23	0.38
15	4.9	1.29	0.39
20	3.81	1.3	0.39

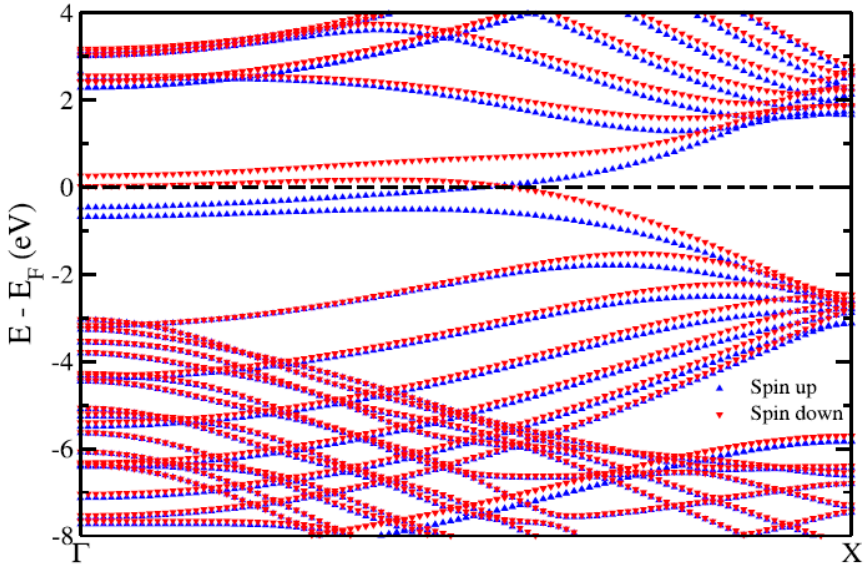

Despite the absence of dangling bonds...

Magnetism at zigzag edges V

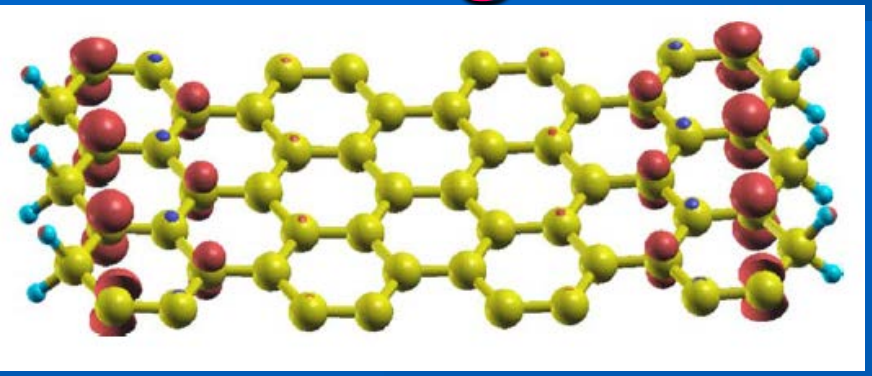

Magnetization density

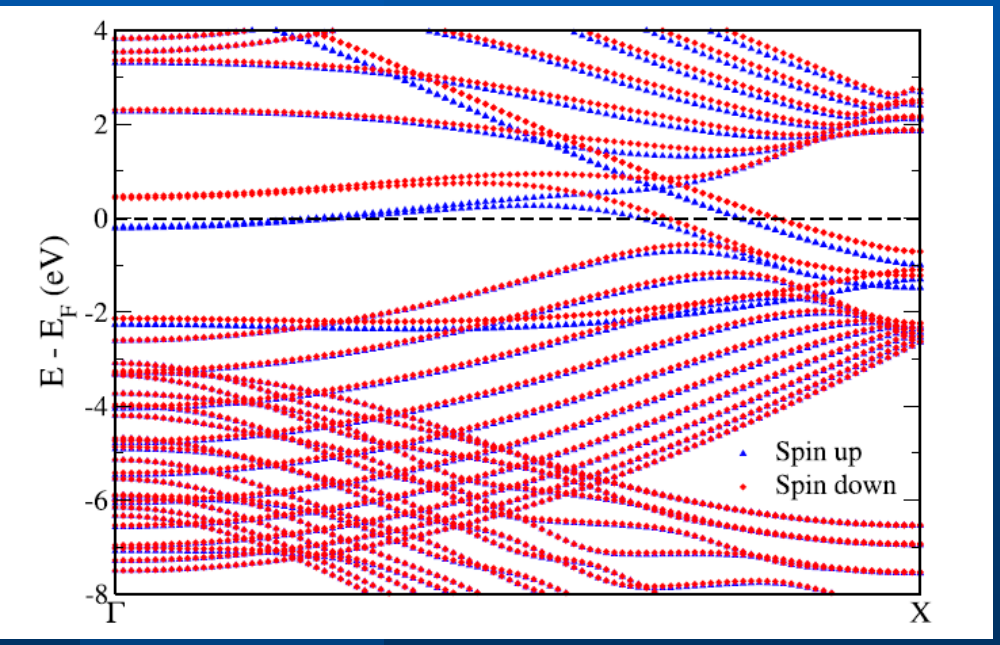

The model: just cut off double-hydrogenated carbon atoms

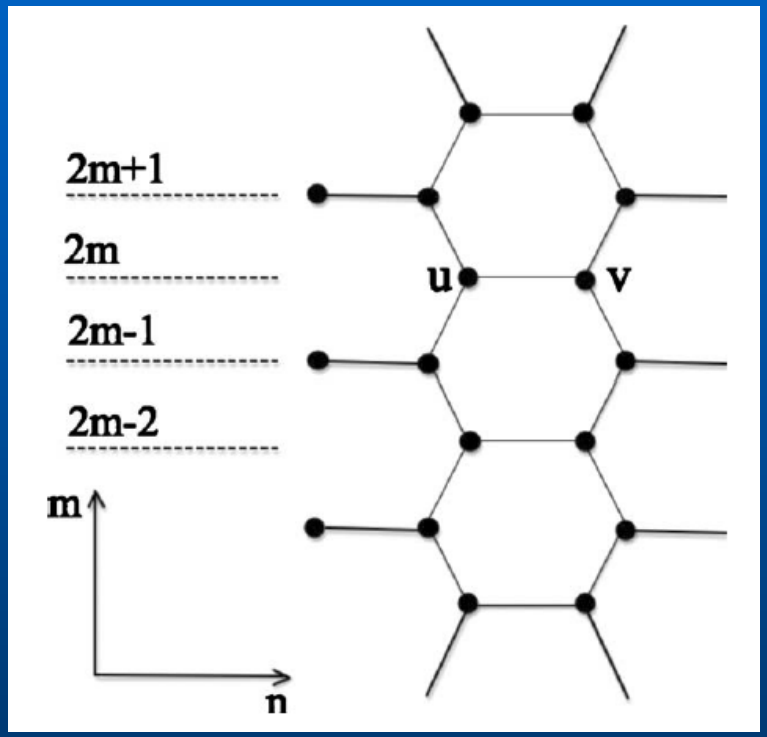

Zero-energy mode appears!

Spin-polarized bands in carbon-terminated nanoribbons

Dangling bonds in grain boundaries

Akhukov, Fasolino, Gornostyrev & MIK, PR B 85, 115407 (2012)

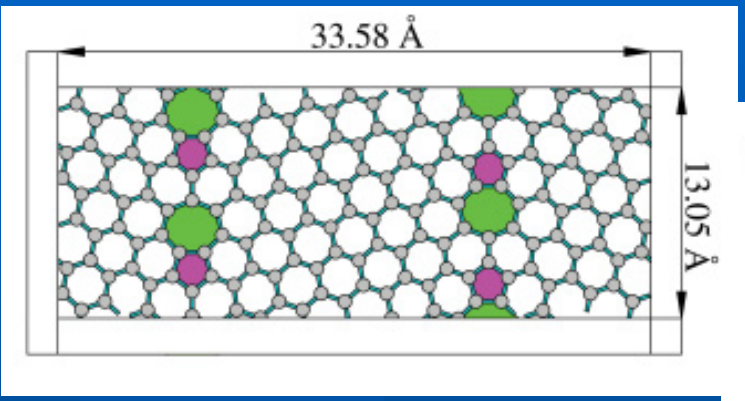

57 defect is nonmagnetic

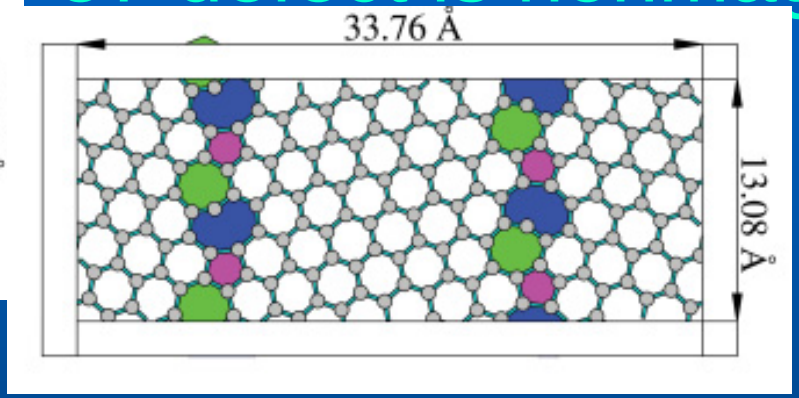

587 Magnetic and typical

And more...

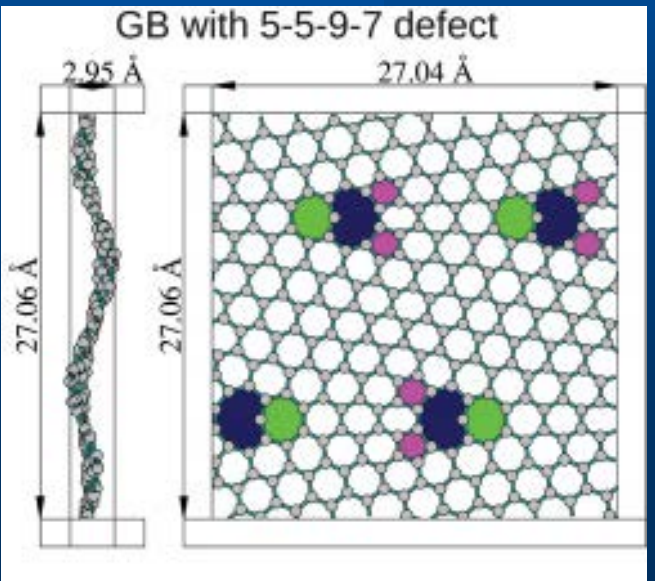

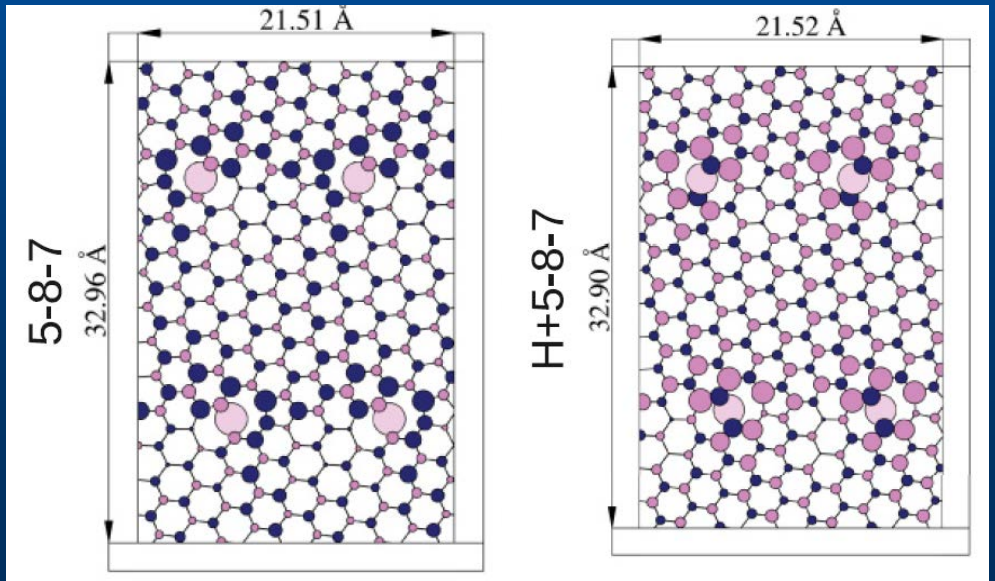

Spin density

Carbon foams

Akhukov, MIK & Fasolino, J. Phys.: Cond. Mat. 25, 255301 (2013)

24,000 configurations; about 1% have magnetic moments

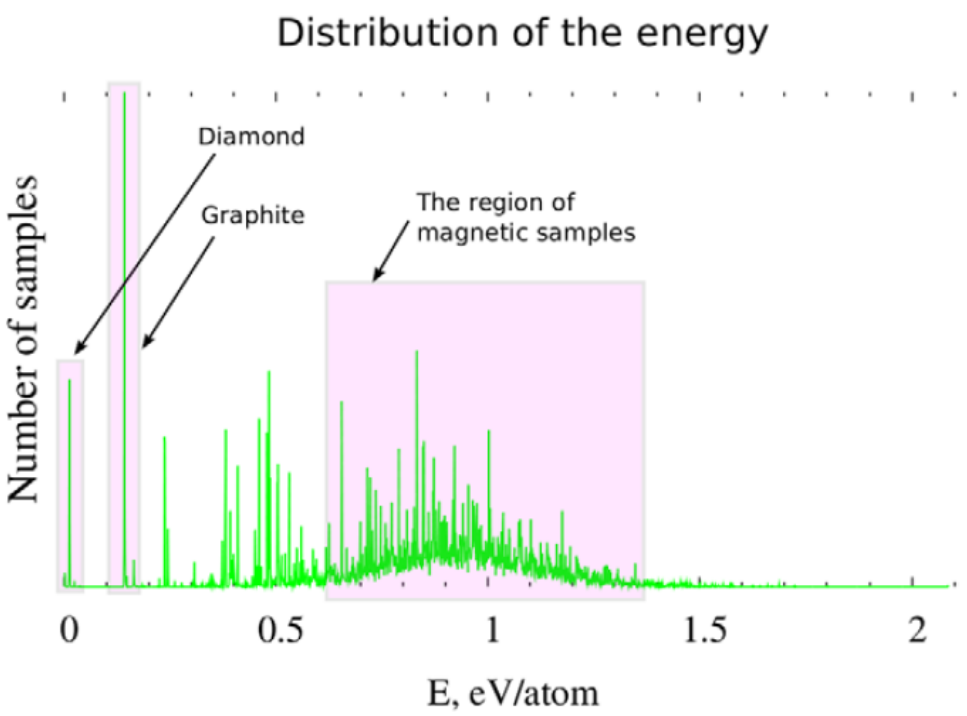

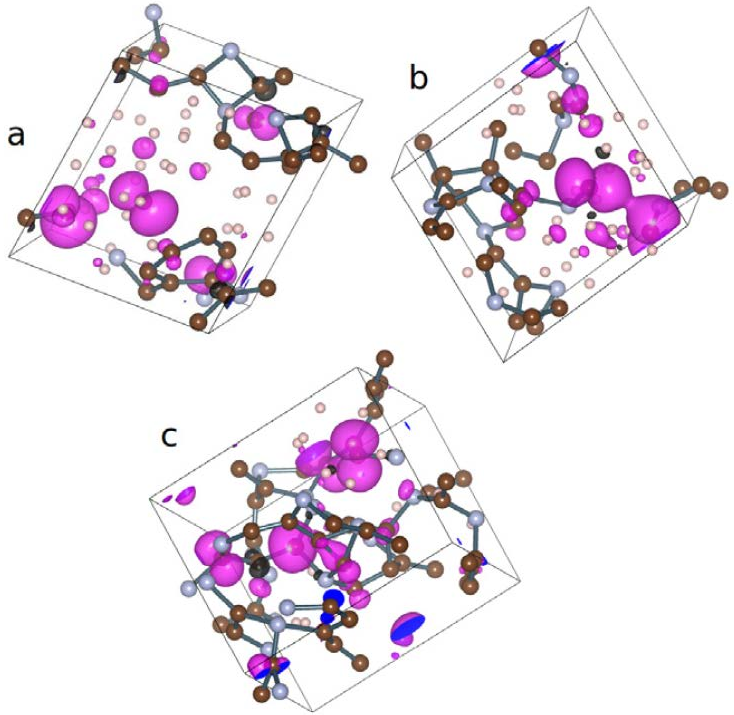

Exchange interactions in concentrated systems: C_2H and C_2F

PHYSICAL REVIEW B **88**, 081405(R) (2013)

Exchange interactions and frustrated magnetism in single-side hydrogenated and fluorinated graphene

A. N. Rudenko,[1,*] F. J. Keil,[1] M. I. Katsnelson,[2] and A. I. Lichtenstein[3]

Two-side fluorinated or hydrogenated graphene is nonmagnetic. Single-side: claim for FM

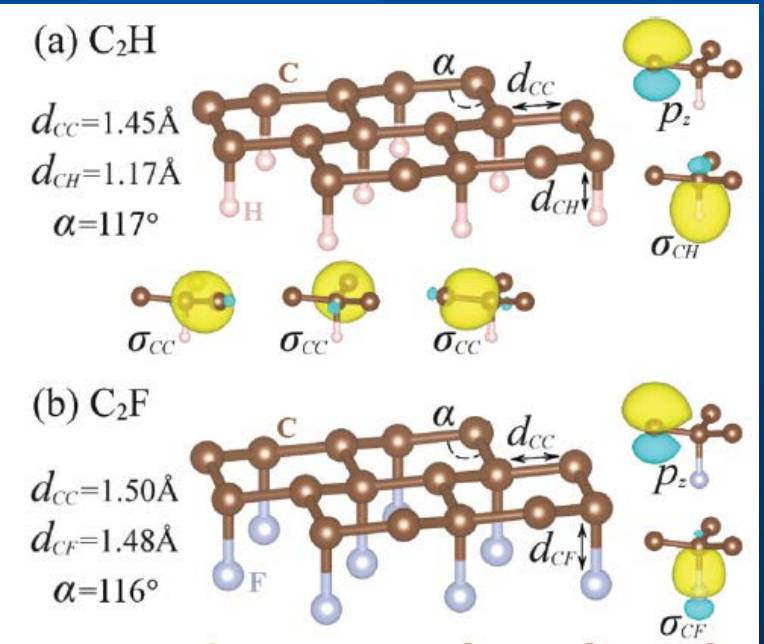

Structure, orbitals, nonmagnetic bands

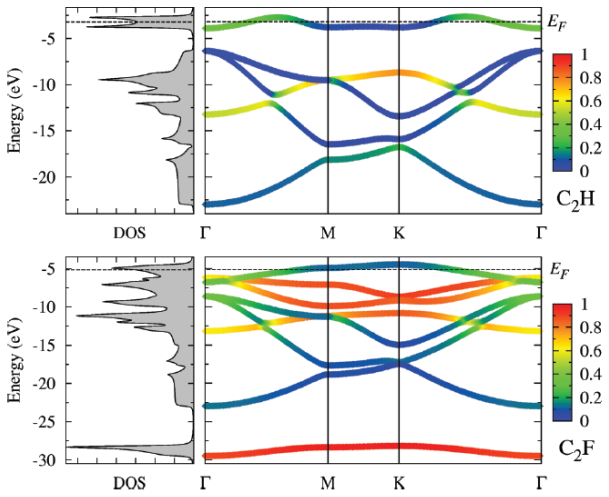

FIG. 2. (Color online) Band structure and density of states (DOS) for C_2H and C_2F obtained from non-spin-polarized calculations. Contributions from the impurity orbitals (*s* for H and *sp* for F) are shown by color.

C_2F and C_2H II

Mapping on classical Heisenberg model (A. Lichtenstein & MIK)

$$H = -\sum_{i \neq j} J_{ij} \mathbf{s}_i \cdot \mathbf{s}_j$$

$$J_{ij}^{\alpha\beta} = \frac{1}{4\pi} \int_{-\infty}^{E_F} d\varepsilon \, \mathrm{Im}\left[\Delta_\alpha G_{ij}^{\alpha\beta\downarrow}(\varepsilon) \Delta_\beta G_{ji}^{\beta\alpha\uparrow}(\varepsilon)\right]$$

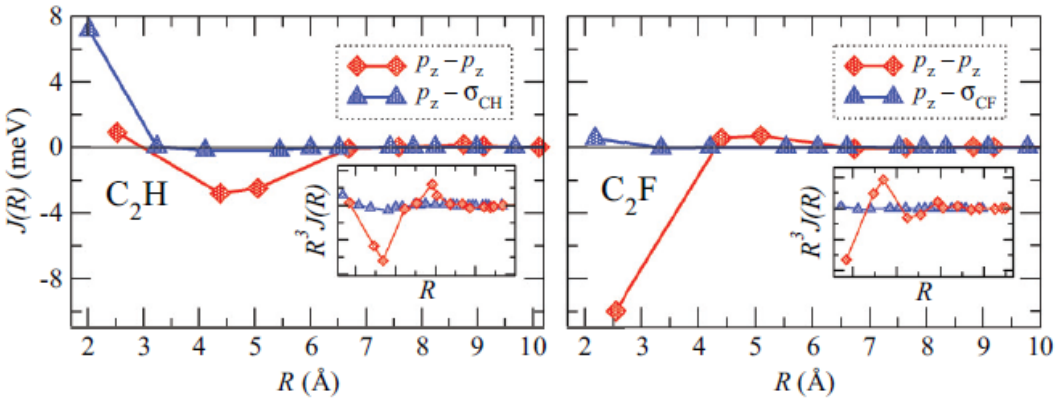

Well-localized magnetic moments

Quantum effects: Quantum spin liquid?!

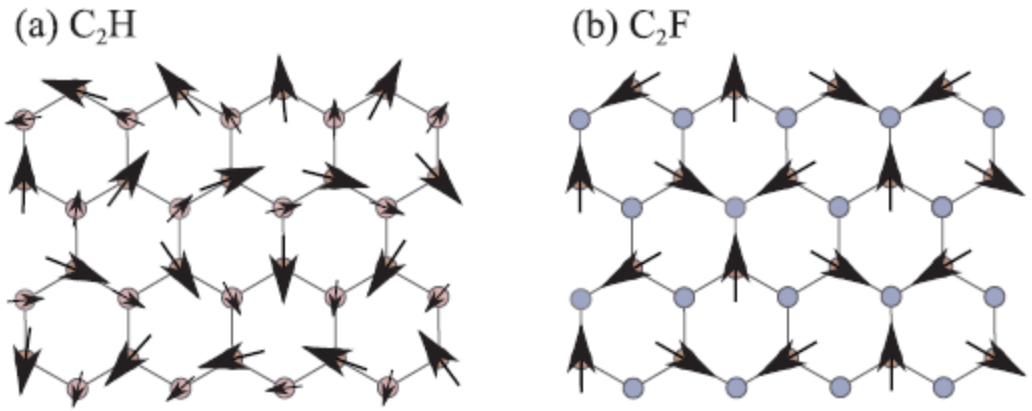

FIG. 5. (Color online) Spin structures corresponding to a classical ground state for (a) C_2H (incommensurate spin spiral) and (b) C_2F (120° Néel state).

C_2H and C_2F III

PHYSICAL REVIEW B **94**, 214411 (2016)

Role of direct exchange and Dzyaloshinskii-Moriya interactions in magnetic properties of graphene derivatives: C_2F and C_2H

V. V. Mazurenko,[1] A. N. Rudenko,[1,2] S. A. Nikolaev,[1] D. S. Medvedeva,[1] A. I. Lichtenstein,[1,3] and M. I. Katsnelson[1,2]

Not the end of story!

Direct exchange is important and make C_2H ferromagnetic!

Spin-orbit coupling is not negligible

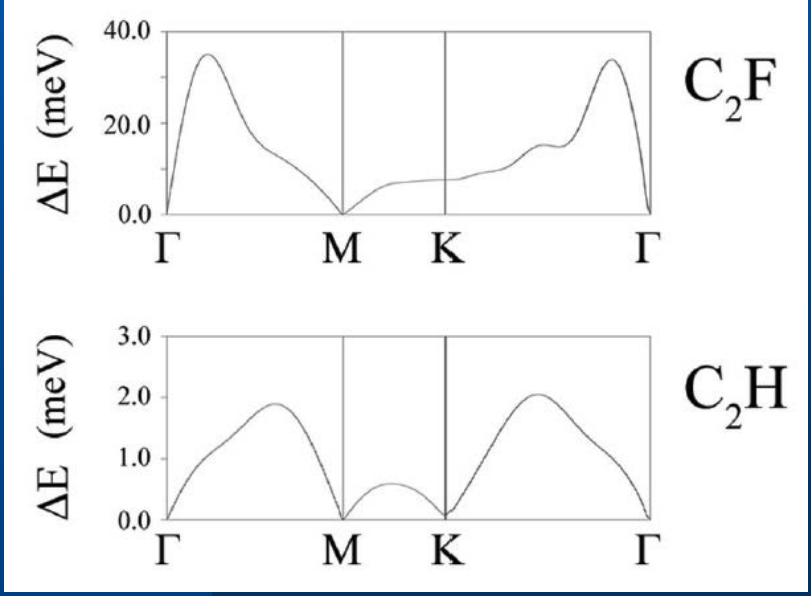

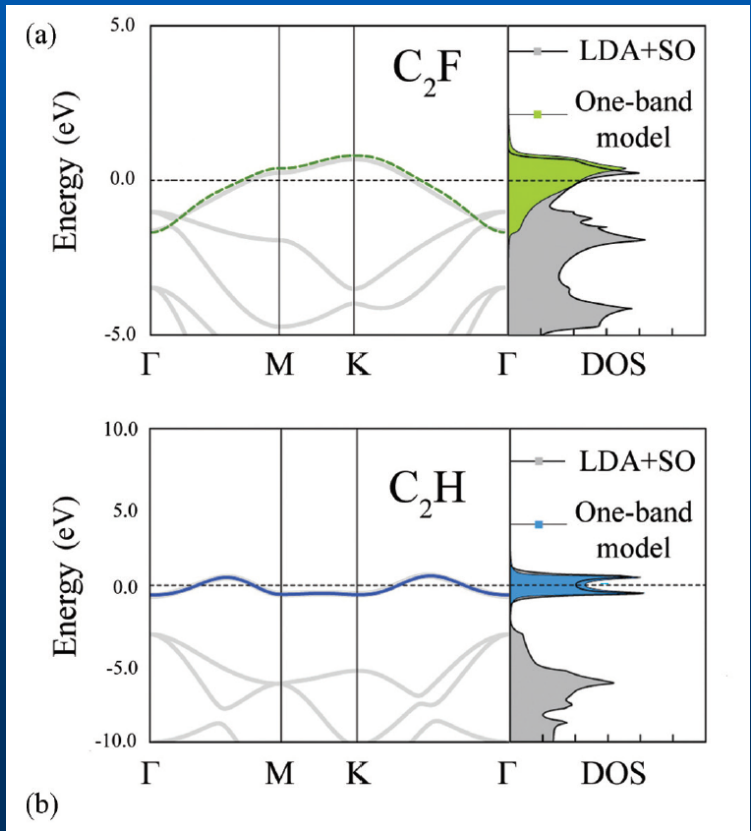

C_2H and C_2F IV

Coulomb interaction is strong: Mott insulators

TABLE II. The calculated local and nonlocal partially screened Coulomb interactions (in eV) for C_2F and C_2H. The two values of J_{01}^F correspond to the fully screened and bare interactions.

Interaction	C_2F	C_2H
U_{00}	5.16	4.69
U_{01}	2.46	2.19
U_{02}	1.66	1.11
U_{03}	1.46	0.85
J_{01}^F (screened)	0.018	0.034
J_{01}^F (bare)	0.044	0.099

C_2H and C_2F V

DM interactions are quite noticeable for C_2F

For C_2F 1 meV, for C_2H 10 μeV

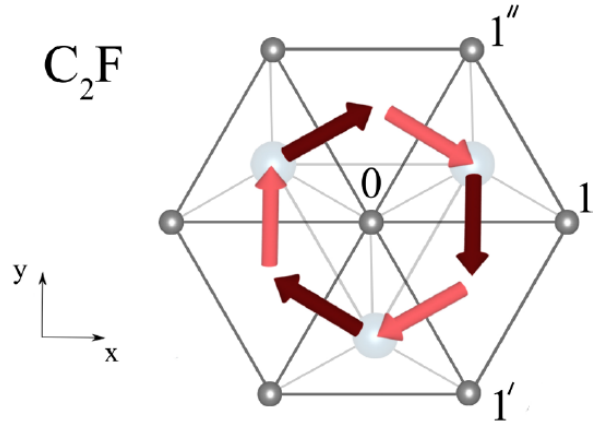

FIG. 4. Schematic representation of the Dzyaloshinskii-Moriya vectors in C_2F. Light and dark red arrows denote the Dzyaloshinskii-Moriya vectors with positive and negative z components, respectively.

Skyrmion lattice at high magnetic field: C_2H

$\frac{T}{|J_{01}|} = 0.02$ $\frac{B}{|J_{01}|} = 0.1$ $J_{01}^F > 40$ meV

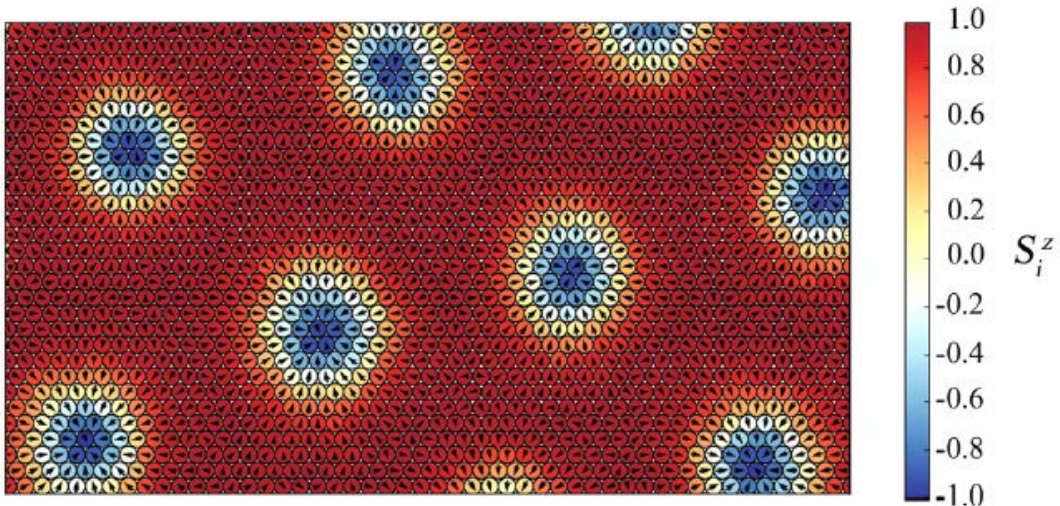

$g = 2.025$ for C_2F

25 Å

Conclusions

- sp electron magnetic semiconductors can be better than conventional – if one finds FM...
- local magnetic moments is not a problem but FM is; even when one has strong exchange it is not necessarily FM
- very unclear situation for magnetism at the edges (beyond the talk)
- very interesting and unusual sp-electron strongly correlated magnetic systems C_2H and C_2F

Main collaborators

M.Akhukov, A.Fasolino, A.Rudenko (Nijmegen)
A.Geim, I.Grigorieva, K.Novoselov (Manchester)
D.Edwards (London)
O.Yazyev (Lausanne)
A.Lichtenstein (Hamburg)
T.Wehling (Bremen)
M.Ulybyshev (Regensburg)
V.Mazurenko (Ekaterinburg)
D.Boukhvalov (Seoul)
O.Eriksson, B.Sanyal (Uppsala)

MANY THANKS!